

VORTEX SHEDDING FROM A STEP-CYLINDER IN SHEAR FLOW

Warren Dunn

Stavros Tavoularis

Department of Mechanical Engineering,
University of Ottawa
Ottawa, ON K1N 6N5, Canada
stavros.tavoularis@uottawa.ca

ABSTRACT

Vortex shedding patterns behind a step-cylinder in uniformly shear flow for Reynolds numbers between 152 and 674 were studied using flow visualization and laser Doppler velocimetry. The results were analyzed using spectral analysis and the wavelet transform. The effect of shearing on vortex shedding was found to be significant. As in uniform flow, the step-change in diameter caused the formation of a distinct near-step vortex cell behind the large cylinder, with frequency lower than those in both neighbouring cells. Shearing affected both the spanwise length of this cell and the difference between its frequency and that in the adjacent large-cylinder cell. The values of these parameters were found to depend both on the Reynolds number and the orientation of the cylinder axis relative to the shear direction.

INTRODUCTION

Flows past bluff objects, and the resulting forces on them, are topics of great interest in many engineering applications. Significant insight in such flows can be achieved by examining the relatively simple case of uniform flow past circular cylinders, a subject which has received very intense interest (Zdravkovich, 1997; 2003). Nevertheless, in the majority of practical problems, the object is geometrically complex and the surrounding stream is spatially variable, and sometimes time-dependent as well. Such flows possess features not present in the previously mentioned simple paradigm and are dependent on both the geometrical and the dynamic complexities. To gain insight into the various interacting mechanisms, it seems worthwhile to examine a sequence of problems such that non-uniformities in the object's cross-section and the flow are introduced independently and in a controlled manner.

In most technological and environmental flows past elongated immersed objects, the velocity varies along the span of the object, a condition commonly referred to as shearing. The magnitude of shear also generally varies, as for example in the case of boundary layers. To simplify this problem, one may consider the idealized case of uniformly sheared flow (USF), in which the mean flow velocity varies linearly in the direction normal to the stream. It is well

known (Griffin, 1985; Zdravkovich, 1997) that, if a two-dimensional bluff object is placed with its axis parallel to the velocity gradient, it will shed frequencies in a cellular fashion along its span, such that the shedding frequency would be constant within each cell, but change from one cell to the other, increasing in the direction of the velocity gradient. Maull and Young (1973) were among the first to identify this phenomenon, by examining USF past an object with a semi-elliptical nose followed by a rectangular section. The local Strouhal number in cellular vortex shedding, based on the local free stream velocity at each spanwise location, varies continuously within each cell and changes abruptly across cell boundaries such that its difference from the Strouhal number in uniform flow at comparable values of the local Reynolds number does not exceed certain bounds. Previous investigators have demonstrated that the size of spanwise cells depends on the shear magnitude, the aspect ratio of the object and the use of endplates to terminate the object in the stream (Mair and Stansby, 1975; Rooney and Peltzer, 1981; Tavoularis et al., 1987; Anderson and Szewczyk, 1995).

Besides shear, another source of complexity in vortex shedding patterns is non-uniformity in the object's cross-sectional shape and/or area. Once more, it would be instructional to consider first objects with geometrically simple cross-sectional changes, such as tapered cylinders and step-cylinders, including finite ones. The wakes of such objects in uniform streams have been documented by several investigators (e.g., Gaster, 1969; Ayoub and Karamcheti, 1972; Williamson, 1989; Lewis and Gharib, 1992; Papangelou, 1992). We have recently documented experimentally cellular vortex shedding from step-cylinders in uniform streams (Dunn and Tavoularis, 2006). This work identified three cells of constant frequency away from the cylinder ends, with abrupt frequency jumps across cell boundaries: the "L-cell", behind the large cylinder and away from the step; the "S-cell" behind the small cylinder; and the "N-cell" behind the large cylinder and near the step, with a frequency lower than that in the L-cell. Near cell boundaries, some vortices connected to one or more co-rotating vortices in the adjacent cell, but others looped around to connect to counter-rotating vortices in the same cell.

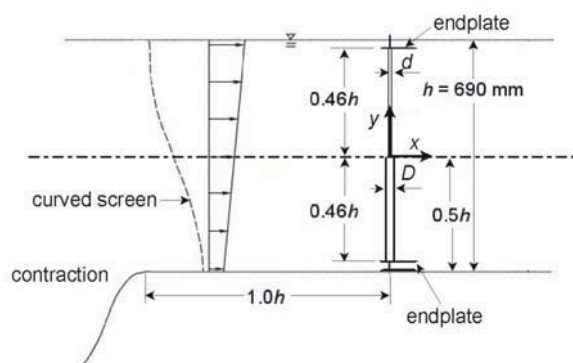


Fig. 1: Sketch of the experimental setup ("inverted" configuration).

The present research is an extension of this previous work, in which a step-cylinder has been inserted in uniformly sheared flow (USF), thus examining, in a relatively simple configuration, vortex shedding in the presence of both cross-sectional and free-stream non-uniformities. Besides the general documentation of such flows, a specific interest is to explore means by which one can predict the combined flow characteristics by superimposing the separate effects of step section change and flow velocity variation.

EXPERIMENTAL FACILITIES AND PROCEDURES

Two stainless steel cylinders with a diameter ratio $d/D = 0.52$ ($D = 6.60$ mm) were co-axially joined at one end ($y = 0$) and placed vertically in a water channel with a water depth of $h = 690$ mm, as illustrated schematically in Fig. 1. The step-cylinder was positioned in either of two vertical orientations, "upright" (with the large cylinder placed above the small one) or "inverted". For comparison purposes, a uniform cylinder with a diameter $d = 3.43$ mm and a length equal to $0.92h$ was also tested in the same flows. The ends of all cylinders were fitted with endplates in an attempt to reduce end effects and were secured either to the bottom of the test section or to a support above the water surface. The cylinders were carefully aligned with the vertical direction and were free of vibrations. For flow visualization purposes, all cylinders were covered by lead foil of thickness 0.13 mm (the foil thickness has been included in the diameters given previously). USF was produced by a curved woven screen with a solidity of 0.59 , made of stainless steel wire with a diameter of 0.38 mm (Dunn and Tavoularis, 2007), such that the velocity increased approximately linearly with increasing y/D .

The local velocity was measured using laser Doppler velocimetry at 116 positions along the cylinder span, approximately 4.5 local diameters (d or D) downstream and 0.78 diameters to the side of each cylinder axis. Typical vertical profiles of the mean streamwise velocity are shown in Fig. 2. The Reynolds number $Re = U_c D / \nu$ (U_c is the velocity at $y = 0$ and ν is the kinematic viscosity of water) was in the range 152 to 674 and the shear parameter $\beta = (h/U_c)(dU/dy)$ varied from 0.265 to 0.506 , depending on the value of Re .

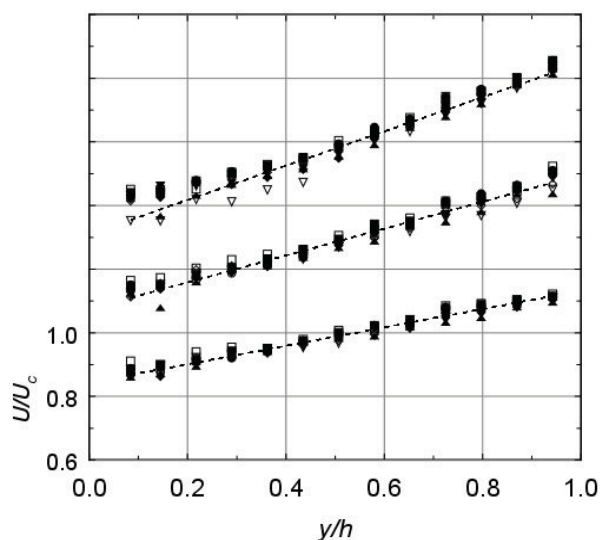


Fig. 2: Freestream mean velocity profiles at $U_c = 29$ mm/s (top), 46 mm/s (middle), and 95 mm/s (bottom); $z/b = -0.26$ (∇), -0.19 (\diamond), -0.11 (\square), -0.04 (\circ), 0.04 (\bullet), 0.12 (\blacksquare), 0.19 (\blacklozenge), 0.27 (\blacktriangledown) and 0.35 (\blacktriangle); --- linear fit to the velocity measurements. The vertical scales of the top and middle profile sets have been shifted upwards by 0.2 and 0.4 units, respectively.

Visualization of the shed vortices was achieved using electrolytic precipitation of the lead foil, which produced a suspension of white tracer particles with diameters of the order of $1\mu\text{m}$ (Taneda et al., 1979). Images were recorded with a digital video camera (Sony DCR-VX1000) at a rate of 30 frames per second.

To produce the evenly spaced time series required for spectral and wavelet analyses, the randomly spaced data provided by the LDV system were resampled at a rate of 25 Hz using the sample-and-hold technique (Adrian and Yao, 1987). Data records of 205 s were acquired at each location. Each record was divided into three blocks with an overlap of 25% and processed by an FFT algorithm, which computed spectra with a frequency resolution of 0.012 Hz.

Space-time analysis of the measured velocity was achieved with the use of the wavelet transform, based on the Morlet wavelet (Farge, 1992; Daubechies, 1992; Torrence and Compo, 1998). The results of the wavelet transform are typically given in the form of iso-contours, plotted against time and Strouhal number. The amplitude of the contours was normalized by its largest value within each plot, to illustrate the relative significance of phenomena recurring at different frequencies, with larger amplitudes indicated by darker shading. The term "amplitude peak" will be used to describe the largest amplitudes, similar to the use of the term "spectral peak" in a power spectrum. Cross-sections of the wavelet map parallel to the Strouhal number axis at a given instant in time may be viewed as "local" frequency spectra, having peaks at dominant local Strouhal numbers.

Additional details about the experimental techniques have been given by Dunn and Tavoularis (2006) and Dunn (2004).

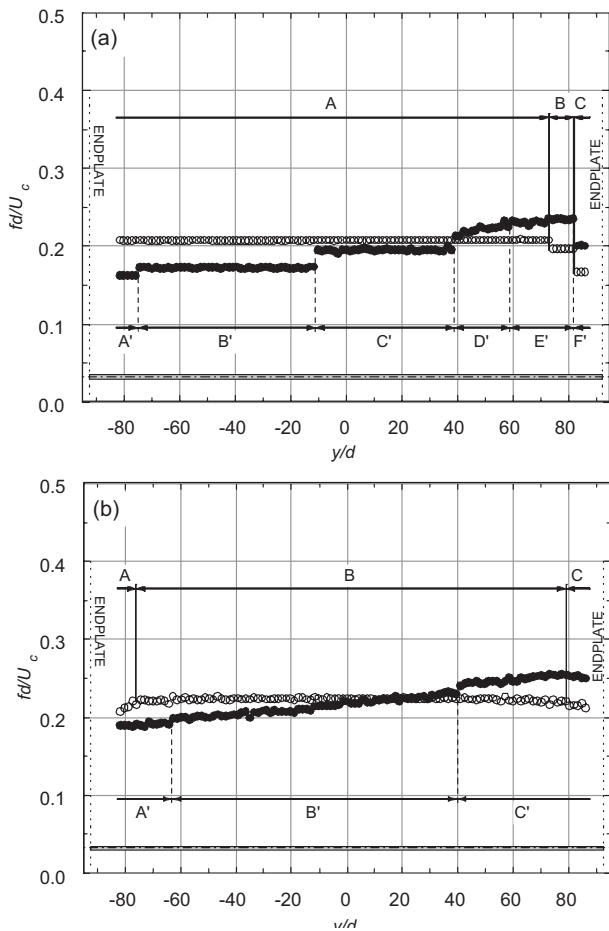


Fig. 3: Dimensionless vortex shedding frequency from a uniform cylinder in uniform (\circ) and shear (\bullet) flow, at $Re = 146$ (a) and 336 (b).

RESULTS AND DISCUSSION

The insertion of any object in a shear flow causes displacement of the mean streamlines towards the low-velocity region, where flow obstruction is lower (e.g., Hall, 1956; Lighthill, 1957; Tavoularis and Szymczak, 1989). When a uniform cylinder is inserted in USF, vortex shedding takes place discontinuously and in a cellular fashion along the cylinder, with the frequency within each cell decreasing towards the low-velocity region. Measurements of the local Strouhal number variation along the span of the uniform cylinder in both uniform flow and in USF are shown in Fig. 3. In uniform flow, along the span of the cylinder and away from the endplates, a single vortex shedding frequency was detected for both $Re = 146$ (cell A in Fig. 3a) and $Re = 336$ (cell B in Fig. 3b), reproducing results that have been documented numerous times. End-cells can also be observed in these figures, most noticeably at the lower Reynolds number. In the shear flow, cellular shedding became obvious at $Re = 146$. Cells A' and F' may be attributed to the endplates, but two distinct cells were observed in the range $-75 < y/d < 39$. The lack of a distinct cell of constant frequency along the upper region of the cylinder may be attributed to the local Reynolds number being in the unstable range of the Re - St curve, in which the

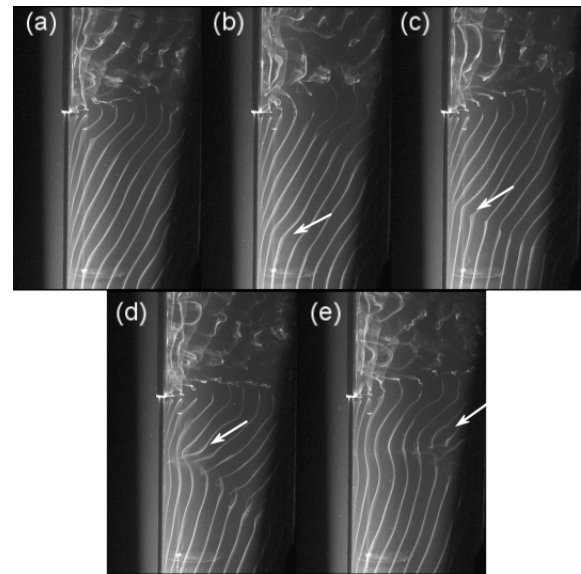


Fig. 4: Cell boundary development in shear flow; $Re = 159$; (a) nearly parallel shedding, (b) a sudden change in vortex inclination, (c) spanwise drift, (d) vortex splitting, (e) streamwise loop formation.

frequency might fluctuate even under constant flow conditions. At locations where the local Reynolds number exceeded the unstable range, cell E' appeared to have a nearly constant frequency, especially towards the upper end of the cylinder. The cellular nature in the shear flow at $Re = 336$ was less clear, but it appeared that three cellular regions may have formed. Cell A' was wider than cells that formed as a result of end effects, as, for example, can be seen by comparison to cell A in the uniform flow case. The shedding frequency in cell B' increased continuously with the increase in flow speed, yet there were frequency jumps at both ends of this cell. For the span $y/d > 40$, the frequency in cell C' also increased continuously, but at a lower rate.

Similar phenomena occur behind each uniform part of a step-cylinder in shear flow, albeit further complicated by the step. The cyclic formation of a cell boundary behind the small half of the step-cylinder in shear flow is illustrated in Fig. 4. Fig. 4a captures an instant during which vortices in two adjacent cells were shed continuously and had a uniform inclination with respect to the free stream direction, in conformity with the varying convection velocity in the shear flow; no cell boundary is discernible at this instant. The formation of a cell boundary was initiated by a sudden change in the inclination of a vortex (Fig. 4b), and the location of the inclination change drifted spanwise towards higher speeds with each subsequent vortex (Fig. 4c). At some instance, a vortex consisting of two sufficiently misaligned sections split, giving rise to streamwise filaments. Filaments from two consecutive vortices shed in the high-speed part of the flow from opposite flanks of the cylinder turned around and joined these vortices in a half-loop (Fig. 4d). Vortices shed subsequently from either side of the cell boundary deflected around the looped pair to be connected continuously (Fig. 4e). The cycle was repeated at the beat frequency, which was approximately equal to the

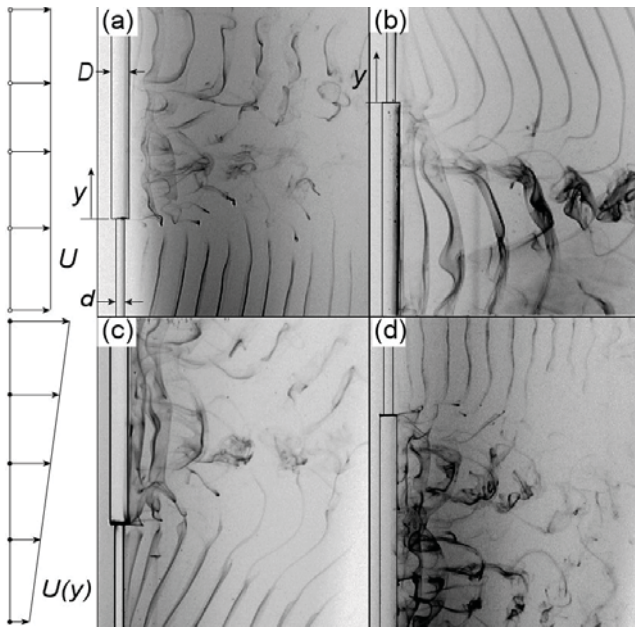


Fig. 5: Vortices in uniform (top) and shear (bottom) flows; Re differed slightly within the range 152 to 168.

difference between the peak shedding frequencies in the two cells.

Figure 5 shows vortex shedding patterns from a step-cylinder in both uniform flow and in USF at comparable Re . In uniform flow, the step-change in diameter distorted the nominal two-dimensionality of the mean stream, displacing streamlines towards the small cylinder, which poses lower obstruction to the stream. Thus, the local streamwise velocity approaching the near-step region behind the large cylinder was lower than that in the free-stream, which gave rise to the N-cell. This cell occurred cyclically, increasing in spanwise length with time and then suddenly collapsing (Dunn and Tavoularis, 2006). The shapes of the N-cell vortices were horseshoe-like, with streamwise half-loops and cross-boundary vortex connections occurring at both cell boundaries. With the “upright” step-cylinder in shear flow, shear-induced streamline displacement was in the same direction as streamline displacement due to the step. As a result, by comparison to the case with the step-cylinder in uniform flow, the N-cell became longer. In the “inverted” configuration, streamline displacement due to shear was in the opposite direction as streamline displacement due to the step, and the N-cell became shorter. Vortices in the shear flow were generally less well-defined than those in corresponding uniform flow cases, exhibiting a stronger waviness along their lengths. Those shed by the large cylinder also contained streamwise finger-like disturbances. In uniform flow, vortices behind the small cylinder were inclined such that their parts shed closest to the step were further downstream than parts shed away from the step. Vortices behind the large cylinder were roughly parallel to those behind the small cylinder, such that their parts shed closest to the step were upstream of parts shed away from the step. In the shear flow, the vortices were convected downstream at speeds increasing with y/D along their spans, so that the inclinations of vortices shed from upright

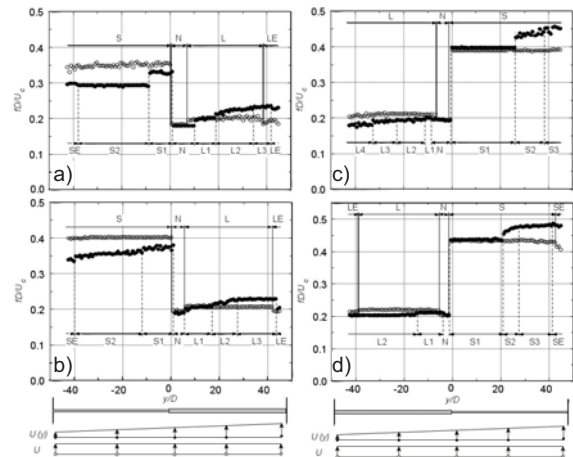


Fig. 6: Local Strouhal number variation along the span of a step-cylinder in uniform (\circ) and shear (\bullet) flows; (a) upright at $Re = 275$, (b) upright at $Re = 625$, (c) inverted at $Re = 294$, and (d) inverted at $Re = 647$.

cylinders increased, while the inclinations of those shed from the inverted cylinders were reversed.

As examples of the available spectral measurements, the spanwise variations of the dominant shedding frequencies behind an inverted step-cylinder in uniform and shear flows have been presented in Fig. 6. The time-averaged locations of the cell boundaries at each spanwise position, based on the occurrence of peaks at the corresponding dominant frequencies, have also been indicated in this figure. Shear generated additional constant-frequency cells along the spans of both cylinders. Away from the step and the free end, two cells ($L1'$ and $L2'$) occurred behind the large cylinder at $Re = 640$, both with frequencies lower than those in uniform flow. The frequency jump between cells $L1'$ and $L2'$ was about 3.6%. Two cells ($S1'$ and $S3'$) also formed behind the small cylinder away from the end, with a frequency jump of about 7.5%. The observed gradual frequency change over a region between these cells (labelled $S2'$) could be attributed to spanwise drifting of the cell boundaries, as seen in flow visualization studies, or might define a distinct, unstable, cell. Vortex connections at the $L1'$ - $L2'$ and $S1'$ - $S2'$ cell boundaries were similar to those observed at the N-cell boundaries in uniform flow.

The effect of shear on the locations of the N-cell boundaries behind upright and inverted cylinders at two Reynolds numbers can be seen in Table 1. Compared to the uniform flow cases, the length of the N-cell increased for upright cylinders, while it decreased for inverted cylinders, at both Reynolds numbers. As seen in Fig. 5, the step discontinuity enforced the location of the N-S cell boundary during vortex formation, but, as the vortices were convected downstream, this boundary was displaced by several diameters toward the large cylinder. Fig. 6 indicates a much smaller displacement at the LDV measurement location, which was laterally off the axis of the cylinder. As also shown in Fig. 6, the shear did not significantly affect the location of the N' - $S1'$ cell boundary but caused a substantial shift of the N' - $L2'$ cell boundary toward higher speed fluid, thus generating corresponding changes in the N' cell length,

as mentioned previously. The frequency jump across the N-L cell boundary was relatively small and subject to considerable uncertainty. In uniform flow, this frequency jump was in the range 6 to 8%. At the same Reynolds number in shear flow, this frequency jump decreased dramatically behind the inverted cylinder and increased measurably behind the upright cylinder.

Table 1: Locations of N-cell boundaries, average N-cell length and dimensionless frequency jump across the N-L cell boundary in uniform (UF) and shear (SF) flows for the upright (U) and inverted (I) cases; $\Delta y = |y_{NS} - y_{NL}|$.

Re		y_{NS}/D	y_{NL}/D	$\Delta y/D$	$(f_L - f_N)/f_L$	
295	U	UF	0.1	6.7	6.6	7.2%
		SF	0.8	9.3	8.5	9.1%
	I	UF	-0.4	-6.6	6.2	6.5%
		SF	-0.2	-3.8	3.6	2.1%
630	U	UF	0.8	5.6	4.8	6.8%
		SF	0.8	6.2	5.4	8.8%
	I	UF	-0.5	-5.3	4.8	8.0%
		SF	-0.5	-3.2	2.7	2.7%

In addition to spectral analysis, space-time analysis of the measured velocity was achieved with the use of the wavelet transform. Two representative sets of results for the step-cylinder in USF at $Re = 289$ are shown in Fig. 7, corresponding to $y/D = -3.9$ (at the step), and in Fig. 8, corresponding to $y/D = 0.0$ (at the N'-L1' cell boundary, see Fig. 6).

At the step, signal modulation was very strong, although the signal had a smaller oscillation amplitude than at other spanwise locations (Fig. 7a). The wavelet map contained amplitude peaks at the frequency associated with vortex shedding from both the large and small cylinders, at Strouhal numbers of 0.196 and 0.405, respectively (Fig. 7b). At this location, the peaks at the lower frequency were higher, and occurred more often, showing that the vortices shed from the large cylinder were not deflected away from the step in this configuration, in contrast to observations for the case of step cylinder in uniform flow. The amplitude of the modulation in the velocity signal was strongest when the wavelet transform peaked at the two dominant frequencies simultaneously, as at $t = 18$ s; the peak at the lower frequency was more pronounced than the one at the higher frequency. There were many more time intervals during which no frequency was dominant; at these times, the velocity signal was usually at its lowest amplitude. As in the uniform flow case, the local frequency of the amplitude peaks varied irregularly with time (Fig. 7c), which is consistent with the continuous change in vortex inclination at the step.

Velocity fluctuations at the boundary between cells N' and L1' of figure 4 were very strong and also had strong modulation (Fig. 8a). The wavelet map showed fewer fluctuations in amplitude in the shear flow (Fig. 8b), than in the uniform flow case. The highest amplitude peaks were more uniform in magnitude over longer durations, and appeared with a nearly regular frequency. Immediately following many of the highest peaks, the amplitude dropped

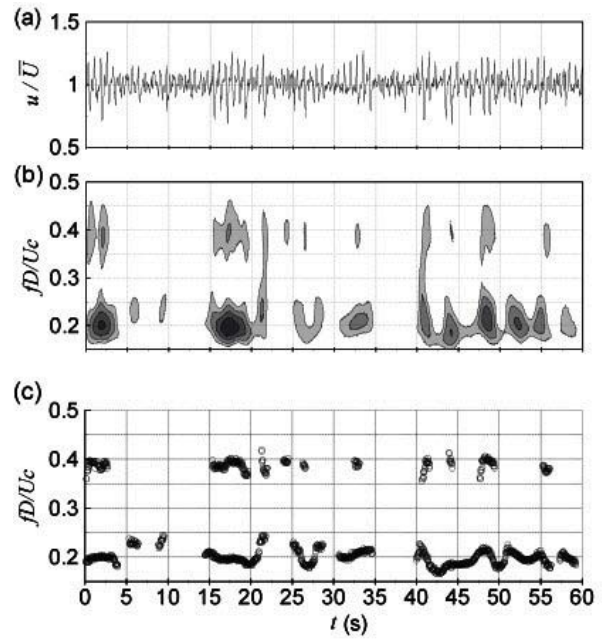


Fig. 7: Inverted step cylinder in shear flow; $y/D = 0.0$ (at the step); $Re = 289$. (a) velocity, (b) wavelet map, and (c) peak local frequency.

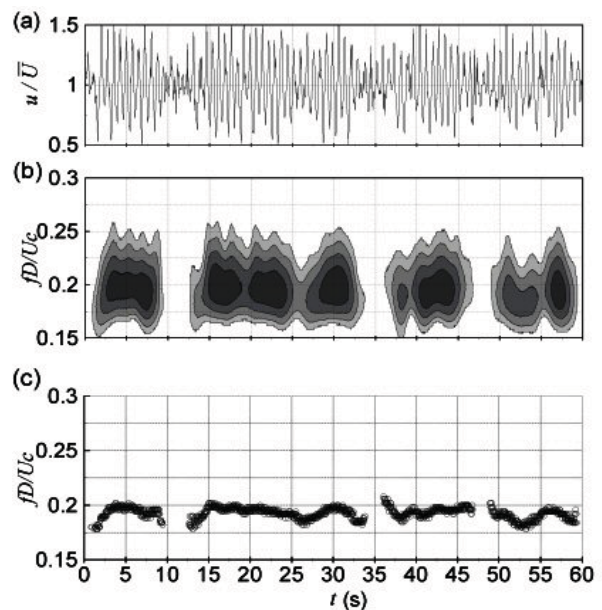


Fig. 8: Inverted step-cylinder in shear flow; $y/D = -3.9$ (near the N-L cell boundary); $Re = 289$; (a) velocity, (b) wavelet map, and (c) peak local frequency.

quickly with time. The frequency band of the amplitude peaks had approximately the same size as that in the uniform flow case. The local frequency of the peaks showed a fluctuation amplitude of nearly half that in the uniform flow case at this location, although the fluctuation period was about the same (Fig. 8c). For comparison, the Fourier spectrum showed peaks at Strouhal numbers of 0.202 and 0.196, respectively. This indicates that the vortices were likely changing inclination, but by a smaller amount than in

the uniform flow. The beat period in this case was 25 s, which was much longer than the observed period.

Behind the small cylinder, far from the step, the shedding frequency did not appear to be affected by the vortices shed from the large cylinder. This was also seen in the spectral analysis and the flow visualization. The wavelet map was similar to the uniform flow case, with little variation in amplitude, and at a frequency that was nearly constant.

CONCLUSIONS

The present study has identified significant effects of freestream shearing on vortex shedding characteristics from a step-cylinder. As in uniform flow, the step-change in diameter caused the formation of a distinct near-step vortex cell behind the large cylinder, with frequency lower than those in both neighbouring cells. Shearing affected both the spanwise length of this cell and the difference between its frequency and that in the adjacent large-cylinder cell. The values of these parameters were found to depend both on the Reynolds number and the orientation of the cylinder axis relative to the shear direction.

ACKNOWLEDGEMENT

The financial support of the Natural Sciences and Engineering Research Council of Canada is gratefully acknowledged.

REFERENCES

- Ayoub, A., and Karamcheti, K., 1982, "An Experiment on the Flow Past a Finite Circular Cylinder at High Subcritical and Supercritical Reynolds Numbers", *J. Fluid Mech.*, Vol. 118, pp. 1-26.
- Adrian, R.J., and Yao, C.S., 1987, "Power Spectra of Fluid Velocities Measured by Laser Doppler Velocimetry", *Exp. Fluids*, Vol. 5, pp. 17-28.
- Anderson, E.A., and Szewczyk, A.A., 1995, "Vortex Shedding from a Straight and Tapered Circular Cylinder in Uniform and Shear Flow", *Proceedings, 6th International Conference on Flow Induced Vibration* (P.W. Bearman, ed.), London, UK, pp. 61-71.
- Daubechies, I., 1992, "Ten Lectures on Wavelets", *CBMS-NSF, Regional Conference Series in Applied Mathematics*, SIAM, Philadelphia, USA.
- Dunn, W., 2004, *Vortex Shedding from Cylinders with Step-Changes in Diameter in Uniform and Shear Flows*, Ph.D. Dissertation, Department of Mechanical Engineering, University of Ottawa, Ottawa, Canada.
- Dunn, W., and Tavoularis, S., 2006, "Experimental Studies of Vortices Shed from Cylinders with a Step-change in Diameter", *J. Fluid Mech.*, Vol. 555, pp. 409-437.
- Dunn, W., and Tavoularis, S., 2007, "The Use of Curved Screens for Generating Uniform Shear at Low Reynolds Numbers", *Exp. Fluids*, Vol. 42, pp. 281-290.
- Farge, M., 1992, "Wavelet Transforms and Their Applications to Turbulence", *Annu. Rev. Fluid Mech.*, Vol. 24, pp. 395-457.
- Gaster, M., 1969, "Vortex Shedding from Slender Cones at Low Reynolds Numbers", *J. Fluid Mech.*, Vol. 38, pp. 565-576.
- Griffin, O.M., 1985, "Vortex Shedding from Bluff Bodies in a Shear Flow: A Review", *J. Fluids Eng.*, Vol. 107, pp. 298-306.
- Hall, I.M., 1956, "The Displacement Effect of a Sphere in a Two-dimensional Shear Flow", *J. Fluid Mech.*, Vol. 1, pp. 142-162.
- Lewis, C.G., and Gharib, M., 1992, "An Exploration of the Wake Three Dimensionalities Caused by a Local Discontinuity in Cylinder Diameter", *Phys. Fluids A*, Vol. 4, pp. 104-117.
- Lighthill, M.J., 1957, "Contributions to the Theory of the Pitot-tube Displacement Effect", *J. Fluid Mech.*, Vol. 2, pp. 493-512.
- Mair, W.A., and Stansby, P.K., 1975, "Vortex Wakes of Bluff Cylinders in Shear Flow", *J. Appl. Math.* Vol. 28, pp. 519-540.
- Maull, D.J., and Young, R.A., 1973, "Vortex Shedding from Bluff Bodies in a Shear Flow", *J. Fluid Mech.* Vol. 60, pp. 401-409.
- Rooney, D.M., and Peltzer, R.D., 1981, "Pressure and Vortex Shedding Patterns Around a Low Aspect Ratio Cylinder in a Sheared Flow at Transitional Reynolds Numbers", *J. Fluids Eng.*, Vol. 103, pp. 88-96.
- Papangelou, A., 1992, "Vortex Shedding from Slender Cones at Low Reynolds Numbers", *J. Fluid Mech.*, Vol. 242, pp. 299-321.
- Taneda, S., Honji, H., and Tatsuno, M., 1979, "The Electrolytic Precipitation Method of Flow Visualization", *Flow Visualization: Proceedings of the International Symposium on Flow Visualization*, (T. Asanuma, ed.), 1977, Tokyo, Japan, pp. 209-214.
- Tavoularis, S., Stapountzis, H., and Karnik, U., 1987, "Vortex Shedding from Bluff Cylinders in Strongly Sheared Turbulent Streams", *J. Wind Eng. and Ind. Aerod.*, Vol. 26, pp. 165-178.
- Tavoularis, S., and Szymczak, M., 1989, "Displacement Effect of Square-ended Pitot Tubes in Shear Flows", *Exper. Fluids*, Vol. 7, pp. 33-37.
- Torrence, C., and Compo, G.P., 1998, "A Practical Guide to Wavelet Analysis", *Bull. Amer. Meteor. Soc.*, Vol. 79, pp. 61-78.
- Williamson, C.H.K., 1989, "Oblique and Parallel Modes of Vortex Shedding in the Wake of a Circular Cylinder at Low Reynolds Numbers", *J. Fluid Mech.*, Vol. 206, pp. 579-627.
- Zdravkovich, M.M., 1997, *Flow Around Circular Cylinders, Vol 1: Fundamentals*, Oxford University Press, New York, USA.
- Zdravkovich, M.M., 2003, *Flow Around Circular Cylinders, Vol 2: Applications*, Oxford University Press, New York, USA.